Available online at www.sciencedirect.com
SCIENCE DIRECT®
ELSEVIER
International Journal of Solids and Structures 42 (2005) 5399–5412
INTERNATIONAL JOURNAL OF SOLIDS and STRUCTURES
www.elsevier.com/locate/ijsolstr

Thermal effects on interfacial stress transfer characteristics of carbon nanotubes/polymer composites

Y.C. Zhang, X. Wang *

Department of Engineering Mechanics, School of Naval Architecture, Ocean and Civil Engineering, Shanghai Jiao Tong University, Shanghai 200240, People's Republic of China

Received 14 July 2004; received in revised form 18 February 2005
Available online 7 April 2005

Abstract

The paper presents an analytical method to investigate thermal effects on interfacial stress transfer characteristics of single/multi-walled carbon nanotubes/polymer composites system under thermal loading by means of thermoelastic theory and conventional fiber pullout models. In example calculations, the mechanical properties and the thermal expansion coefficients of carbon nanotubes and polymer matrix are, respectively, treated as the functions of temperature change. Numerical examples show that the interfacial shear stress transfer behavior can be described and affected by several parameters such as the temperature field, volume fraction of CNT, and numbers of wall layer and the outermost radius of carbon nanotubes. From the results carried out it is found that mismatch of thermal expansion coefficients between the carbon nanotubes and polymer matrix may be more important in governing interfacial stress transfer characteristics of carbon nanotubes/polymer composite system.

Keywords: Carbon nanotubes/polymer composites; Interfacial stress transfer; Thermal loading

1. Introduction

Recently, due to many unique electrical, mechanical and thermal properties of carbon nanotubes (CNTs), a number of theoretical analyses and experiments have been presented in order to study the mechanical characteristics of CNTs/polymer composite structures by Schadler et al. (1998), Bower et al. (1999), Qian and Dicdkey (2000), Fu et al. (2000), Liao and Seam (2001), Lau and Shi (2002), Lau (2003) and Lau et al. (2004). Qian and Dicdkey (2000) gives that the performance of a composite material

* Corresponding author. Tel./fax: +86 2154745367.
E-mail address: xwang@mail.sjtu.edu.cn (X. Wang).

0020-7683/$ - see front matter © 2005 Elsevier Ltd. All rights reserved.
doi:10.1016/j.ijsolstr.2005.02.038

Nomenclature

ρ_0	non-relaxed radius of CNTs [m]
m,n	chiralities of carbon nanotubes
α_N	thermal expansion coefficient of CNTs [°C^{-1}]
α_m	thermal expansion coefficient of polymer matrix [°C^{-1}]
F	pullout force [N]
R_N	outermost radius of CNTs [m]
b	radius of matrix [m]
L	length of CNTs [m]
d	interval spacing of MWNT [m]
h	effective wall thickness of MWNT [m]
N	layer numbers of MWNT
V_{NT}	volume fraction of CNTs
γ	transverse area ratio between the CNTs and matrix
E_{SWNT}	elastic modulus of SWNT [N/m^2]
E_N	elastic modulus of MWNT [N/m^2]
υ_N	Poisson's ratio of CNTs
υ_m	Poisson's ratio of matrix
ΔT	temperature change [°C]
$P_{\max}$	par allowable pull out force [N]

system is critically controlled by the interfacial characteristics of the reinforcement and the matrix material by conducting many experimental investigations. Extensive research has also been given on incorporating different types of CNTs as nano-reinforcements, nano-wires and nano-conductors into polymeric materials to form new composites that possess high mechanical strength, and electrical and thermal conductivity by Ruoff and Lorents (1995, 2003). Lau and Shi (2002) and Lau and Micrcea (2004) describe that in these applications for space and aircraft, one of the anticipated applications of CNTs is ultra-strong reinforcement for high performance composites materials. Lau (2003) has studied the interfacial bonding characteristics of CNTs/polymer composites by using the well-developed local density approximation model (Tu and Yang, 2002), classic elastic shell theory and conventional fiber pullout model (Zhang et al., 1999). Liao and Seam (2001), Lau and Shi (2002) and Lau and Micrcea (2004) also found optimized CNTs/matrix interfacial adhesion results in enhanced strength, toughness, as well as long-term behavior when all the CNTs are parallel to the loading direction in the composite structures.

Based on different views, approaches that were frequently used to investigate the physical and mechanical performances of nano-structures are, generally, (1) the nanometer experimental mechanic such as Li and Bhushan (2002) presented a review of nano-indentation continuous stiffness measurement technique and its applications, and the corresponding useful measurement techniques are used in their investigations on the physical and mechanical characteristics of nanostructures (Li et al., 1997, 1999, 2003, 2004); (2) the molecular dynamic (MD) simulations which have been conducted by several investigators (Yakobson et al., 1996; Belytschko et al., 2002) and (3) the continuum methods of mechanics such as some analytical methods which is used to investigate diffusive shrinkage of a void within a grain of a stressed polycrstal and to solve stability and shrinkage of a cavity in stressed grain (Wang and Li, 2003a,b,c, 2004a,b,c).

It is well known that the interfacial minimal characteristics scale of CNTs-reinforced composites system is about 1–100 nm. As described above, the interfacial mechanical performance of CNTs-reinforced composites system can be investigated by using nanometer experimental mechanics, molecular dynamic (MD)

simulations or continuum methods of mechanics, respectively. Qian and Dicdkey (2000) studied the effect of interfacial adhesive action on strength and toughness of CNTs-reinforced composites systems using TEM image and SEM micrographs. However, it is difficult to qualitatively analyze the initial frictional pull-out force applied on CNTs of CNTs-reinforced composites system directly using the experimental method due to the enhanced strength and very small diameter of the CNTs. MD stimulations is an effective research technique that simulates accurately the physical properties of structures at atomic-scale level. Results from a pullout simulation show that the interfacial shear strength of CNTs/polymer composite system is about 160 MPa (Liao and Seam, 2001), which is much higher than those of most carbon fiber reinforced polymer composites systems. However, the computational problem here is that the time steps involved in the MD simulations are limited by the vibration modes of atoms to be of the order of femto-seconds (10^{-15}). So even after a million time steps, we can reach only the nanosecond range, in which period most of the thermal, mechanical, physical, or magnetic events have not even started (Lau and Micrcea, 2004). For basically computing element of interfacial load transfer in CNTs-reinforced composites system, because the minimum scale of CNTs is 1–100 nm (diameter of CNTs) and minimal characteristics scale of the polymeric matrix is micron scale, it is impractical to perform these simulations on single processor using the MD simulations. Yakobson et al. (1996) solved axial compression buckling problem of SWNT using MD simulations and continuum methods of mechanics, respectively. Comparing the results from the two different methods, it was found that the all-buckling modes achieved by MD simulations could also be predicted by using the continuum methods of mechanics. Authors (Wang and Wang, 2004; Wang et al., 2004, in press) constructed different three dimensional FEM models to obtain an effective bending modulus of CNTs with various rippling deformations.

Besides, Lau and Shi (2002) presents that the thermal expansion of CNTs is fundamentally interesting and technologically important properties. Ruoff and Lorents (1995, 2003) have studied that failure mechanism of carbon CNTs/epoxy composites pretreated in different temperature environments, and addressed that the interaction between the CNTs and matrix consists of electrostatic and van der Waals interaction, deformation induced by these forces, as well as stress/deformation arising from mismatch in the coefficients of thermal expansion. Cooper (2002) described that with the rapid expansion of CNTs composites application, both high strength and high toughness are required in complex working conditions under extreme temperature change environment. Wang and Yang (2005) presented the effect of thermal environment on axially critical load of multi-walled CNTs. However, in the many previous publications, little attention has been paid to investigate thermal effect on the interfacial stress transfer characteristics of CNTs/polymer composites under thermal environments for space applications. Therefore, it is important to understand the thermal effects on interfacial stress transfer characteristics of CNTs/polymer composites under thermal environment.

This paper presents an analytical method to investigate thermal effects on interfacial stress transfer characteristics of single/multi-walled CNTs/polymer composites system under temperature change environments, based on a thermoelastic theory and conventional fiber pullout models (Quek, 2002). In example calculations, the mechanical properties and the thermal expansion coefficients of CNTs and polymer matrix are treated as a function of temperature change. From the results carried out it is found that mismatch for thermal expansion coefficients between the CNTs and polymer matrix may be more important in governing interfacial stress transfer characteristics of CNTs/polymer composite system. Besides, numerical results for the maximum allowable pullout force and the maximum interfacial shear stress under different temperature change environments are obtained for typical single/multi-wall CNTs/polymer composite system.

2. Analytical formulation

A mechanics model of the construction for the pull-out test of an CNTs/ polymer composite under temperature change, ΔT, is shown in Fig. 1. Here, the CNTs with radius R_N and length L is located at

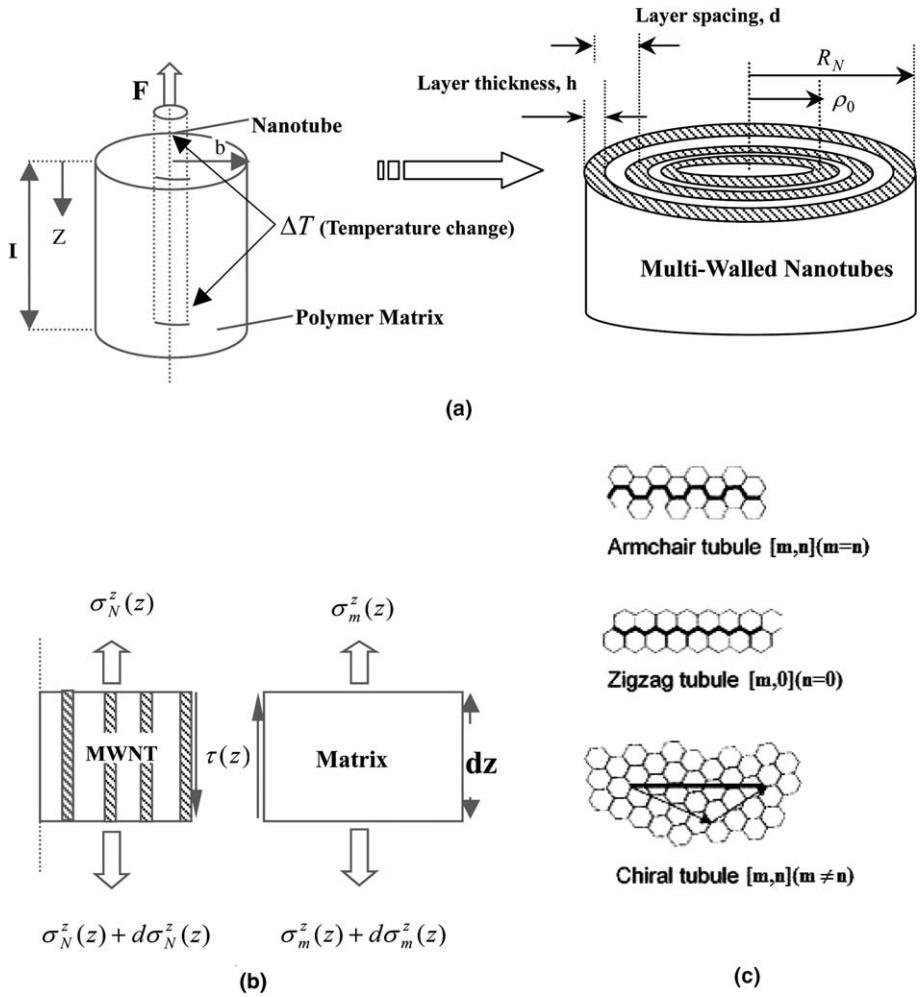

Fig. 1. (a) Schematic diagram of the CNTs/polymer composites under thermal environment; (b) simple fiber pullout model; (c) hexagonal lattice of carbon atoms with different types of chiral vector.

the centre of a co-axial cylindrical polymer matrix with an outer radius b. The multi-walled carbon nanotubes (MWNT) could be imagined as a group of co-axial circular shells packed together with uniform interval spacing d and the effective wall thickness h of the single-walled carbon nanotubes (SWNT). The effective cross-sectional area of the CNTs can be expressed as (Tu and Yang, 2002)

$$A_{\text{eff}} = 2\pi h\left\{N\rho_0 + \sum_{c=1}^{N} d(c-1)\right\} \tag{1}$$

where the non-relaxed radius, ρ_0, is written as

$$\rho_0 = \frac{\sqrt{3(m^2+n^2+mn)}}{2\pi}a_0 \tag{2}$$

In the above formula, N expresses the layer numbers of MWNT, ρ_0, m, n, *and* a_0 are, respectively, the non-relaxed radius and chiralities of the SWNT and C–C bond distance (1.42 Å). The parameter d expresses the

spacing between each graphene layer (≈3.4 Å), the effective wall thickness h of the SWNT is about 3.4 Å. According to the effective stiffness, $Eh = 360$ J/m^2 (Yakobson et al., 1996), the corresponding effective elastic modulus is $E = 1.1$ TPa. The outermost radius of the MWNT as shown in Fig. 1 could be expressed as

$$R_N = \rho_0 + d(N-1) \tag{3}$$

Because the role of the CNTs in advanced composite structures is to take up all stresses that are transferred from the matrix through the interfacial shear stress (Lau and Shi, 2002; Lau et al., 2004), a well-known classical fiber pullout model was used to study the interfacial stress transfer problem of CNTs/polymer composites system and three dimensional, axial-symmetric cylindrical thermoelastic model was proposed to analyze the stress transfer characteristics.

Based on thermoelastic theory, the physical relationships between the stresses and strains in CNTs or in polymer matrix, under thermal environment, are expressed as (Timoshenko and Goodier, 1970)

$$\begin{aligned}
\varepsilon_j^r &= \frac{\partial u_j^r}{\partial r} = \frac{1}{E_j}\left[\sigma_j^r - \upsilon_j(\sigma_j^z + \sigma_j^\theta)\right] + \alpha_j \Delta T_j \\
\varepsilon_j^\theta &= \frac{\partial u_j^r}{r} = \frac{1}{E_j}\left[\sigma_j^\theta - \upsilon_j(\sigma_j^r + \sigma_j^\theta)\right] + \alpha_j \Delta T_j \\
\varepsilon_j^z &= \frac{\partial u_j^z}{\partial z} = \frac{1}{E_j}\left[\sigma_j^z - \upsilon_j(\sigma_j^r + \sigma_j^\theta)\right] + \alpha_j \Delta T_j
\end{aligned} \tag{4}$$

where superscripts, r, θ and z, are used to denote the components of stresses and strains in the cylindrical coordinate axes and the subscript, j, may be N which represents the physical relationship of CNTs or may be m which represents the physical relationship of polymer matrix.

In the above formula, E_N, α_N E_m and α_m are, respectively, express Young's modulus and thermal expansion coefficients of CNTs and polymer matrix, under temperature change environments, which may be a function of temperature change as follows (Mallick, 1997; Shen, 2001)

$$\begin{aligned}
&E_N = E_N^0(1 - 0.0005\Delta T), \quad E_m = E_m^0(1 - 0.0003\Delta T) \\
&\alpha_N = \alpha_N^0(1 + 0.002\Delta T), \quad \alpha_m = \alpha_m^0(1 + 0.001\Delta T)
\end{aligned} \tag{5}$$

where E_N^0, α_N^0 E_m^0 and α_m^0 are, respectively, express elastic modulus and thermal expansion coefficients of CNTs and polymer matrix, under a room temperature environment. The Young's modulus E_N^0 of CNTs estimated by using the local density approximation model and elastic shell theory is written as (Tu and Yang, 2002)

$$E_N^0 = \frac{N}{N - 1 + R} E_{\mathrm{SWNT}}^0 R \tag{6}$$

where R expresses the thickness to spacing ratio of the CNTs (h/d) and E_{SWNT}^0 expresses Young's modulus of SWNT under room temperature environment. It is noted that for $N = 1$, the $E_N^0 = E_{\mathrm{SWNT}}^0$.

From the mechanics model of the construction as shown in Fig. 1, the equilibriums equations between the matrix axial stress, CNTs axial stress and interfacial shear stress are expressed as

$$\frac{\mathrm{d}\sigma_m^z(z)}{\mathrm{d}z} = \frac{2\gamma}{R_N}\tau(z) \tag{7}$$

$$\frac{\mathrm{d}\sigma_N^z(z)}{\mathrm{d}z} = -\frac{2}{R_N}\tau(z) \tag{8}$$

where $\gamma = R_N^2/(b^2 - R_N^2)$ expresses a transverse area ratio between the CNTs and matrix. The external surface conditions of the matrix are written as

$$\sigma_m^r(b,z) = 0, \quad \tau_m^{rz}(b,z) = 0 \tag{9}$$

From Fig. 1 it is seen that the total embedding length of the CNT is L, and because the CNTs is undertaking a pullout force, F, due to the existence of crack opening the axial stress applied on the other end where $z = L$ equals zero. Thus, the two end conditions of this CNTs/polymer composite model are

$$\sigma_N^z(0) = \sigma_{\text{pullout}}, \quad \sigma_N^z(L) = 0 \tag{10}$$

$$\sigma_m^z(0) = 0, \quad \sigma_m^z(L) = \gamma\sigma_{\text{pullout}} \tag{11}$$

where $\sigma_{\text{pullout}} = F/A_{\text{eff}}$.

At the interface, the radial stress and displacements of the CNTs and matrix should satisfy

$$\sigma_m^r(R_N, z) = \sigma_N^r(R_N, z), \quad u_m^r(R_N, z) = u_N^r(R_N, z) \tag{12}$$

Because the MWNT is considered as an effective solid cylinder here, the circumferential and radial stresses in the CNT are identical as follows

$$\sigma_N^r(r, z) = \sigma_N^\theta(r, z), \quad 0 \leqslant r \leqslant R_N \tag{13}$$

Utilizing Eqs. (4), (7), (8), (9), (12) and (13), and following the some solving procedure in early works (Zhang et al., 1999), the axial equilibrium equation for the CNTs under thermal environment is expressed as

$$\frac{d^2\sigma_N^z(z)}{dz^2} - A_1\sigma_N^z(z) = A_2\sigma_{\text{pullout}} + A_3\sigma^{\text{T}} \tag{14}$$

where the parameters of $A_3 = \frac{2k+1}{U_2 - 2kU_1}H$, $H = \frac{(\alpha_N - \alpha_m)\alpha}{\alpha_m}$ and $\sigma^{\text{T}} = E_N\alpha_N\Delta T$ are relation to the thermal loading.

Solving Eq. (14) and utilizing the boundary conditions at the two ends of the CNTs/polymer composite model, Eq. (10), the CNTs axial stress in the completely bonded region is expressed as

$$\sigma_N^z(z) = \omega_1(\sigma_{\text{pullout}})\sinh(\lambda z) + \omega_2(\sigma_{\text{pullout}})\cosh(\lambda z) - \left(\frac{A_2}{A_1}\sigma_{\text{pullout}} + \frac{A_3}{A_1}\sigma^{\text{T}}\right) \tag{15}$$

Substituting Eq. (15) into Eq. (8), the CNTs interfacial shear stress in the completely bonded region is given by

$$\tau(R_N, z) = \frac{-R_N\lambda}{2}[\omega_1(\sigma_{\text{pullout}})\cosh(\lambda z) + \omega_2(\sigma_{\text{pullout}})\sinh(\lambda z)] \tag{16}$$

where the parameters of A_1, A_2, λ, ω_1 (σ_{pullout}) and ω_2 (σ_{pullout}) are the functions of the mechanical properties and geometrical factors of the CNTs and matrix under thermal environments, and are listed in Appendix A.

It is well known that the maximum shear stress should be located at the starting point of pullout end where $z = 0$ (Liao and Seam, 2001). Therefore, substitution of $\tau(0) = \tau_{\max}$ into Eq. (16), the allowable pull out force, $P_{\max} = A_{\text{eff}}\sigma_{\text{pullout}}$, which is the maximum applied force to maintain the CNTs and polymer matrix in contact with each other, can be given by Appendix A

$$P_{\max} = \frac{A_{\text{eff}}\left\{2\tau_{\max}\sinh(\lambda L) + [1 - \cosh(\lambda L)]\frac{A_3}{A_1}\sigma^{\text{T}}R_N\lambda\right\}}{\left[\left(1 + \frac{A_2}{A_1}\right)\cosh(\lambda L) - \frac{A_2}{A_1}\right]R_N\lambda} \tag{17}$$

The corresponding maximum tension stress, $\sigma_{\max}^*$, in the CNTs/polymer composites system under thermal loading is written as

$$\sigma^*_{\max} = \frac{P_{\max}}{A_{\text{eff}}} V_{NT} + \sigma^*_m (1 - V_{NT}) \tag{18}$$

where σ^*_m expresses the axial stress in the polymer matrix when the axial stress in CNTs equals $P_{\max}/A_{\text{eff}}$, and is given by

$$\sigma^*_m = \gamma \left(\frac{P_{\max}}{A_{\text{eff}}} - \sigma^z_N \right) \tag{19}$$

where, $V_{NT} = A_{\text{eff}}/\pi b^2$ expresses the volume fraction of CNTs.

In the above formula, the maximum interface shear stress $\tau_{\max}$ where a CNTs was pulled out from a CNTs/polymer system, has been determined to be 160 MPa through molecular simulation (Liao and Seam, 2001).

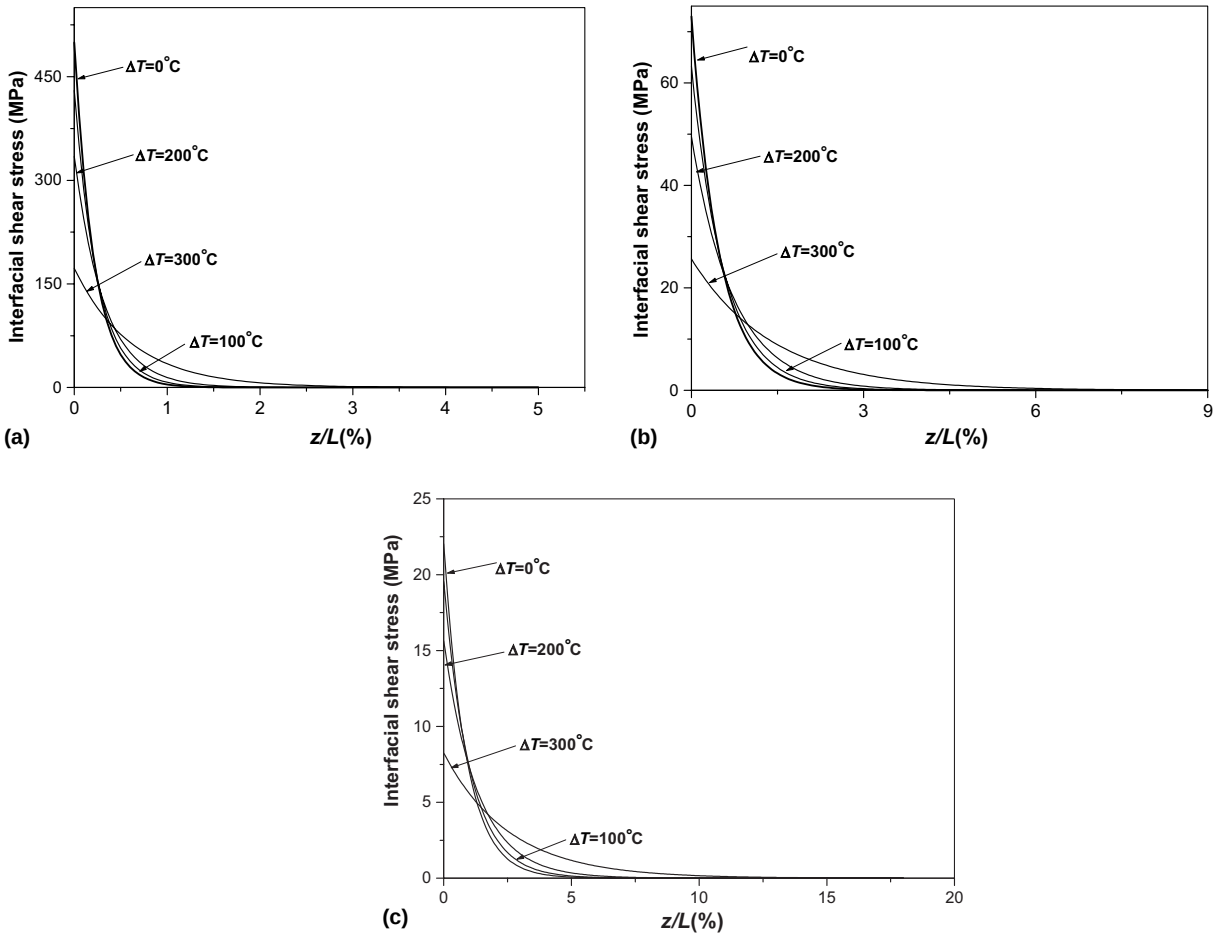

Fig. 2. The distributions of interfacial shear stress, $\tau(R_N, z)$, along axial coordinate, z/L. Where chiral vector of CNTs, $(m,n) = (5,5)$; ΔT expresses the magnitudes of temperature change; N expresses layer numbers of the CNTs, which are (a) $N = 1$, (b) $N = 5$, (c) $N = 10$, respectively.

3. Numerical calculations and discussions

The interfacial shear stress in CNTs/polymer matrix composite system is a critical parameter controlling the efficiency of stress transfer and some of the important mechanical properties of composite such as effective Young's modulus, tensile strength and fracture toughness. Hence, numerical calculations are given for a hypothetical CNTs/epoxy composite system to illustrate the interfacial shear stress transfer mechanism under thermal loading. However, the analysis is equally applicable to other types of CNTs-composite system. The material properties and geometrical characteristics of the CNTs, matrix and interface are shown as (Mallick, 1997; Shen, 2001)

$$h = 3.4\ \text{Å}, \quad d = 3.4\ \text{Å}, \quad b = 2 \times 10^3 \text{nm}, \quad \upsilon_m = 0.48, \quad \upsilon_N = 0.34, \quad E_m^0 = 3.3\ \text{GPa},$$
$$E_{\text{SNT}} = 1.1\ \text{TPa}, \quad a_0 = 1.42\ \text{Å}, \quad L = 1.0 \times 10^4\ \text{nm}, \quad F = 10\ \text{nN},$$
$$\alpha_N^0 = -1.5 \times 10^{-6}\ ^\circ\text{C}^{-1}, \quad \alpha_m^0 = 45 \times 10^{-6}\ ^\circ\text{C}^{-1}$$

Fig. 2 shows distributions of interfacial shear stress $\tau(R_N, z)$ in a CNTs/Epoxy composite system along dimensionless axial distance z/L for different temperature change, ΔT, environments. From Fig. 2(a)–(c), it is seen that the maximum interfacial shear stress between the CNTs and matrix, at $z/L = 0$, gradually decreases as the magnitude of temperature change ΔT increases. The reasons may be attribute to that the volume contraction ratio of CNTs is larger than the volume expansion ratio of epoxy matrix because CNTs is more sensitive to change of temperature subject to the same magnitudes of temperature change. Undoubtedly, the change of volume ratio weakens interactions between CNTs and matrix such as adhesion and interlocking. According to the trend of the curves shown in Fig. 2, the maximum interfacial shear stress is mainly affected by mismatch of thermal expansion coefficient and the Young's modulus between the CNTs and matrix.

From Fig. 2, it is also seen that the transfer length of interfacial shear stresses under different thermal environments significantly decreases as layer numbers of CNTs increase. Because of the larger cross-sectional area of the MWNT with 10 layers, the total surface contact area at the bond interface of MWNT

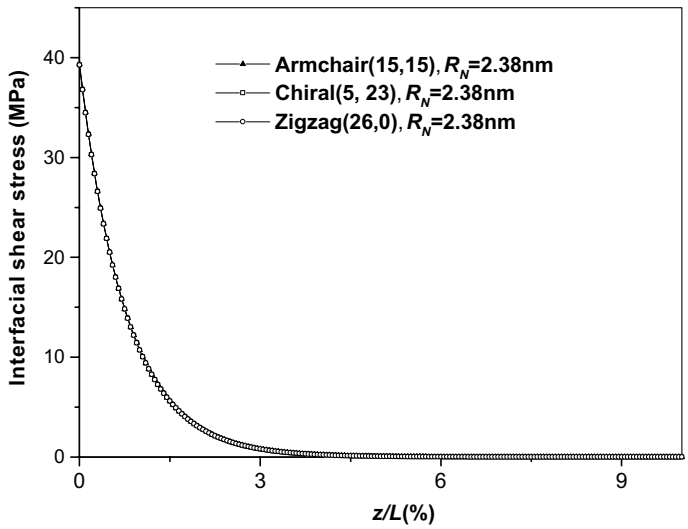

Fig. 3. The distributions of interfacial shear stress, $\tau(R_N, z)$, along axial coordinate, z/L. Where chiral vector of CNTs, is (15, 15),(5, 23) and (26, 0), respectively; the layer numbers of CNTs, $N = 5$; the magnitude of temperature change, $\Delta T = 100\ ^\circ\text{C}$.

with 10 layers is therefore much larger than that of SWNT with 1 layer and MWNT with 5 layers, so that the maximum interfacial shear stress decreases as the layer numbers of CNTs increases. Due to thermal residual interfacial shear stress produced by mismatch in thermal expansion coefficients between CNTs and matrix, the transfer length of interfacial shear stresses increases as the magnitude of temperature change increases. Hence, for a structural stiffness point of view, the existence of the interfacial thermal residual shear stress may be have an advantage of avoiding cracking and fracture at the bond interface, to a large extent.

Fig. 3 shows the distribution of interfacial shear stresses of different chiralities SWNT with identical outermost radius, $R_N = 2.38$ nm, under various thermal environments. It is seen in Fig. 3 that the distributions of interfacial shear stresses of different chiralities SWNT with the same outermost radius are identical.

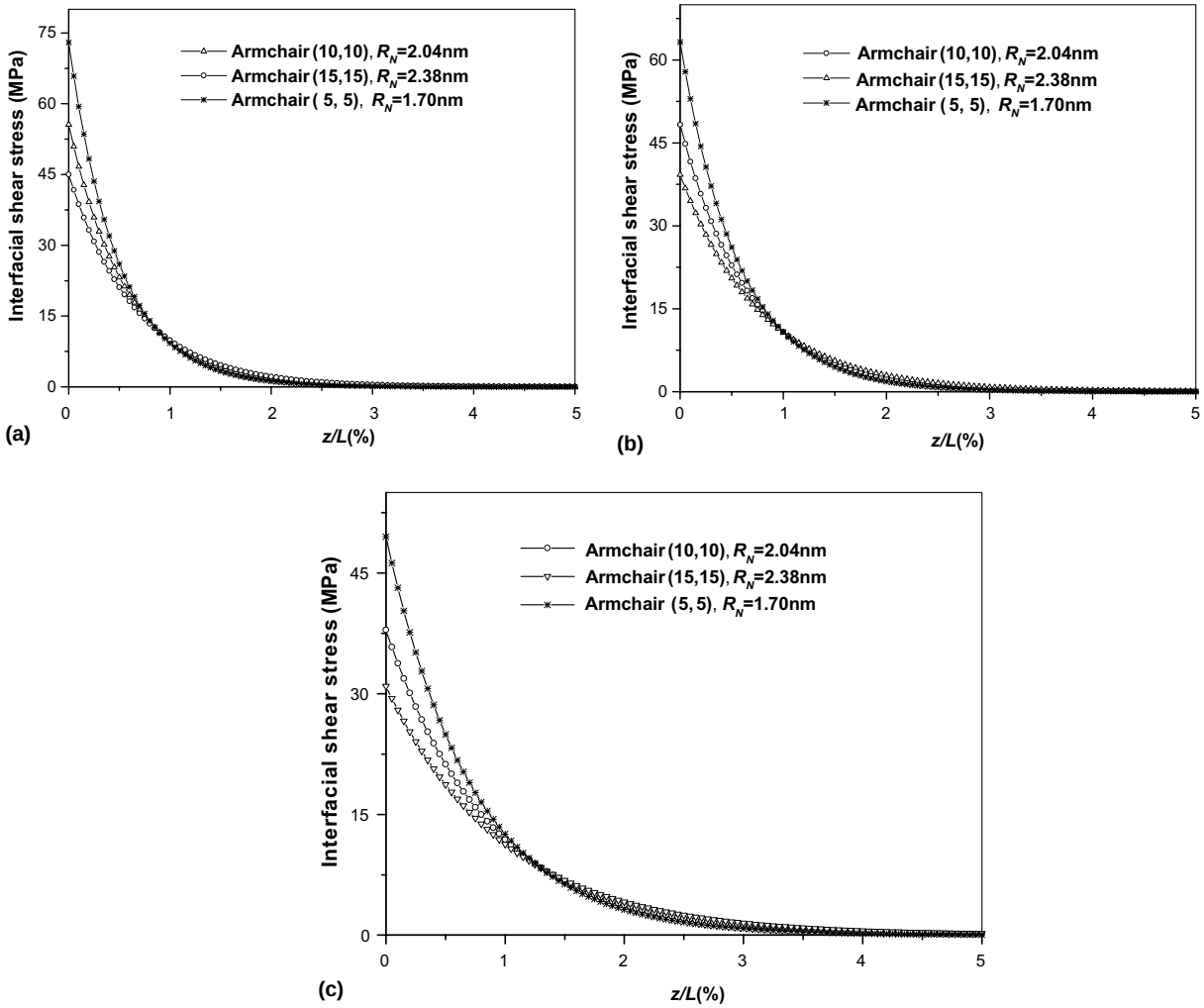

Fig. 4. The distributions of interfacial shear stress, $\tau(R_N, z)$, along axial coordinate, z/L. Where chiralities (m, n) of armchair CNTs, are (15,15),(10,10),(5,5), respectively; the layer number of CNTs, $N = 5$; ΔT expresses the magnitudes of temperature change, which are (a) 0 °C, (b) 100 °C, (c) 200 °C respectively.

Fig. 4 shows that the stress transfer length in the Armchair MWNT/polymer composite system increases as the outermost radius of MWNT and the magnitude of temperature change increases due to interaction of clamping surface stress to the CNTs and frictional force, and the maximum interface shear stress in the Armchair MWNT/polymer composite system decreases as the outermost radius of MWNT and the magnitude of temperature change increase. Comparing Figs. 3 and 4, because CNTs is considered as isotropic properties in the paper, the maximum interfacial shear stress and the shear stress transfer length of MWNT/polymer composite system are independent on the chirality vector of CNTs, but are dependent on the outermost radius of CNTs.

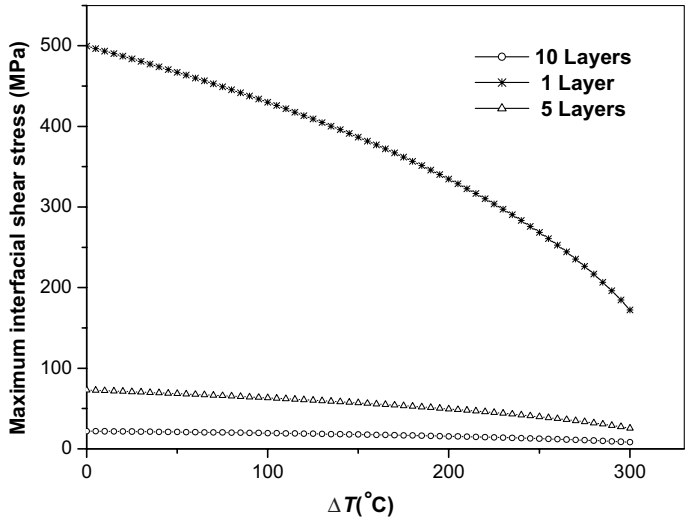

Fig. 5. The distributions of the maximum interfacial shear stress, $\tau_{\max}(R_N, 0)$, for temperature changes. Where chiral vector of the CNTs, $(m,n) = (5,5)$; the layer numbers of CNTs, N, are 1, 5, 10, respectively.

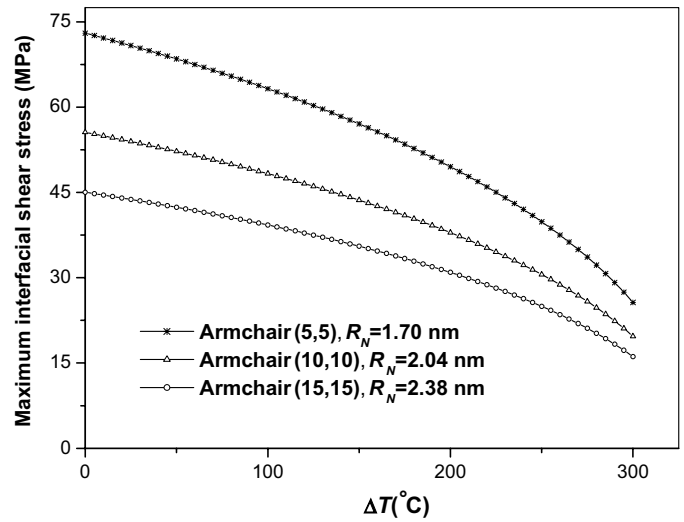

Fig. 6. The distributions of the maximum interfacial shear stress, $\tau_{\max}(R_N, 0)$, for temperature changes. Where the layer number of CNTs, $N = 5$, and chiralities (m,n) of armchair CNTs, are (15, 15), (10, 10), (5, 5), respectively.

The distribution of the maximum interfacial shear stress in MWNT is shown in Fig. 5. It is seen that the thermal effects on the maximum interfacial shear stress in CNTs decreases as the layer numbers of CNT increases. Fig. 6 shows that Armchair CNTs with different outermost radii appear in different effects on the maximum interfacial shear stress of the CNTs under temperature change environments, and the maximum interfacial shear stress of the three types of CNTs decreases as the increasing of temperature change because of the existence of reinforced interfacial adhesion and interlocking produced by thermal residual shear stress.

The distribution of maximum pullout force, $P_{\max}$, for the armchair CNTs with different layer numbers, under various thermal environments is shown in Fig. 7. It is seen that the allowable pullout force of CNTs increases as the increasing of the layer numbers of CNTs and the magnitudes of temperature change.

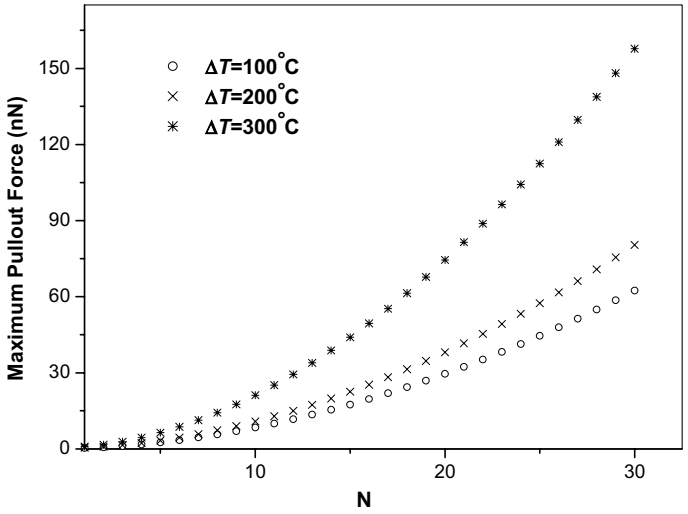

Fig. 7. The distributions of maximum pullout force, $P_{\max}$, for layer numbers of CNTs, N. Where chiral vector of CNTs, $(m,n) = (5,5)$, and ΔT expresses the magnitudes of temperature change.

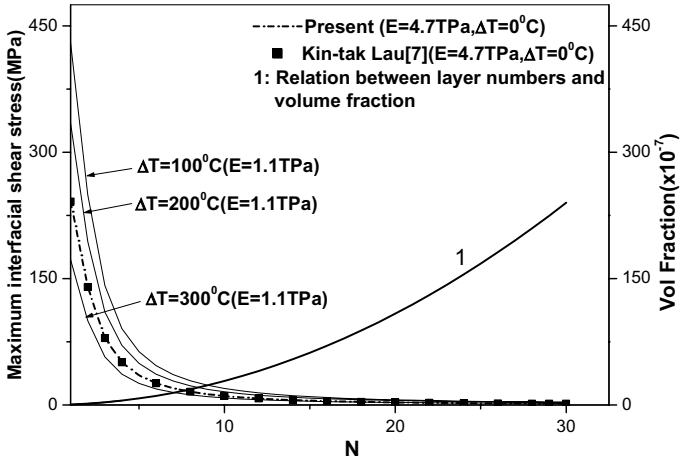

Fig. 8. The distributions of the maximum interfacial shear stress and the volume fraction of CNTs for layer numbers of the CNTs, N. Where chiral vector of the CNTs, $(m,n) = (5,5)$, and ΔT expresses the magnitudes of temperature change.

Fig. 8 shows that distribution of the maximum interfacial shear stress and the volume fraction of CNTs for the layer numbers of CNTs. It is seen that increasing the layer numbers of CNTs could eventually reduce the maximum interfacial shear stress, so that the interfacial bonding strength between the CNTs and matrix is reinforced. It can be seen that the volume fraction of CNTs appears in non-linear increase as the layer numbers of CNTs increase. From Fig. 8 it is also seen that the distributions of the maximum interfacial shear stress and the volume fraction of CNTs no considering temperature change is the same as the literature (Lau, 2003).

4. Conclusions

In this paper, interfacial stress transfer characteristics of CNTs/polymer composites under thermal environments have been presented and discussed. According to analytical results, mismatch in thermal expansion coefficients and Young's modulus between CNTs and matrix may be more important in governing interfacial characteristics of the CNTs/polymer composite system subjected to thermal loading. It is noted that interfacial stress transfer characteristics of CNTs/polymer composites is obviously different from that of fiber reinforced composite system in the literature (Zhang et al., 1999). Results carried out show that increasing of the magnitudes of temperature change will cause some significant phenomena as follows:

(1) decreasing the maximum interfacial shear stress so that to enhance of interfacial strength;
(2) increasing stress transfer length, and to allow stress to be fully transferred from the matrix to the CNTs;
(3) increasing of maximum pullout force and to reduce the possibility of that CNTs is pulled out from the CNT/polymer composite system;
(4) thermal effects on the maximum interfacial shear stress of SWNT/polymer composite system is much larger than that of MWNT/polymer composite system;
(5) because CNTs is considered as isotropic properties in the paper, the maximum interfacial shear stress and the shear stress transfer length of CNTs/polymer composite systems are independent on the chirality vector of CNTs, but are dependent on the outermost radius of CNTs.

In the present study, some results are similar to the experimental data (Schadler et al., 1998) relative to pullout and fragmentation of CNTs/polymer composite system no considering thermal effects. Current work can provide helpful information for describe the stress transfer mechanism of CNTs/polymer composites under thermal loading, which has not been previously discussed elsewhere.

Acknowledgments

The authors thank the referees for their valuable comments.

Appendix A

$$R_{NT} = \rho_0 + d(N-1), \quad \sigma_{\text{pullout}} = \frac{F}{A_{\text{eff}}} \tag{A.1}$$

$$A_1 = \frac{\alpha(1-2k\upsilon_N) + \gamma(1-2k\upsilon_m)}{U_2 - 2kU_1)}, \quad A_2 = -\gamma(1-2k\upsilon_m)/(U_2 - 2kU_1) \tag{A.2}$$

$$k = \frac{\alpha\upsilon_N + \gamma\upsilon_m}{\alpha(1-\upsilon_N) + 1 + 2\gamma + \upsilon_m} \tag{A.3}$$

$$\alpha = \frac{E_m}{E_N}, \quad \eta_1 = \frac{2(1+\upsilon_m)}{\upsilon_m}, \quad \eta_2 = \frac{(1+2\upsilon_m)}{\upsilon_m} \tag{A.4}$$

$$U_1 = \frac{\gamma}{8}\left\{2\eta_1 b^2 \ln\left(\frac{b}{R_N}\right)\left[1+\gamma\left(\frac{b^2}{R_N^2}+1\right)\right] - 2\eta_2\left(b^2+R_N^2\right) + 4b^2 - 2\eta_1\left(b^2-R_N^2\right)\right\} \tag{A.5}$$

$$U_2 = \frac{\gamma\upsilon_m}{4}\left\{2\eta_1 b^2 \ln\left(\frac{b}{R}\right)(1+\gamma) - \eta_2\left(b^2+R_N^2\right) + 2b^2 - \eta_1\left(b^2-R_N^2\right)\right\} \tag{A.6}$$

$$\lambda = \sqrt{A_1}, \quad \gamma = \frac{R_N^2}{b^2-R_N^2} \tag{A.7}$$

$$\omega_1(\sigma_{\text{pullout}}) = \frac{\left(\frac{A_2}{A_1}\sigma_{\text{pullout}} + \frac{A_3}{A_1}\sigma^{\text{T}}\right) - \left[\left(1+\frac{A_2}{A_1}\right)\sigma_{\text{pullout}} + \frac{A_3}{A_1}\sigma^{\text{T}}\right]\cosh(\lambda L)}{\sinh(\lambda L)} \tag{A.8}$$

$$\omega_2(\sigma_{\text{pullout}}) = \left(1+\frac{A_2}{A_1}\right)\sigma_{\text{pullout}} + \frac{A_3}{A_1}\sigma^{\text{T}} \tag{A.9}$$

$$\xi = \alpha(1-\upsilon_N) + 1 + 2\gamma + \upsilon_m \tag{A.10}$$

References

Bower, C., Rosen, R., Jin, L., 1999. Deformation of carbon nanotubes in nanotubes–polymer composites. Applied Physics Letters 74 (22), 3317–3329.

Belytschko, T., Xiao, S., Schatz, G., Ruoff, R., 2002. Atomistic simulation of nanotube fracture. Physical Review B 65, 235430.

Cooper, C.A., 2002. Detachment of nanotubes from a polymer matrix. Applied Physics Letters 81 (20), 3873–3875.

Fu, S.Y., Yue, C.Y., Hu, X. et al., 2000. Analyses of the micromechanics of stress transfer in single- and multi-fiber pull-out tests. Composites Science and Technology 60, 569–579.

Lau, K.T., 2003. Interfacial bonding characteristics of nanotube/polymer composites. Chemical Physics Letters 370, 399–405.

Lau, K.T., Micrcea, C., 2004. On the effective elastic moduli of carbon nanotubes for nanocomposite structures. Composites Part B: Engineering 35, 95–101.

Lau, K.T., Shi, S.Q., 2002. Failure mechanisms of carbon nanotube/epoxy composites pretreated in different temperature environments. Carbon 40, 2965–2968.

Lau, K.T., Chong, G., Gao, G.H. et al., 2004. Stretching process of single-and multi-walled carbon nanotubes for nanocomposite applications. Carbon 42, 423–460.

Li, X., Bhushan, B., 1999. Micro/nanomechanical and tribiological characterization of ultrathin amorphous carbon coatings. Journal of Materials Research 14, 2328–2337.

Li, X., Bhushan, B., 2002. A review of nanoindentation continuous stiffness measurement technique and its applications. Materials Characterization 48, 11–36.

Li, X., Diao, D., Bhushan, B., 1997. Fracture mechanisms of thin amorphous carbon films in nanoindentation. Acta Materialia 45, 4453–4461.

Li, X., Gao, H., Catherine, J., 2003. Nanoindentation of silver nanowires. Nano Letters 3, 1495–1498.

Li, X., Chang, W.C., Chao, Y.J., Wang, R., Chang, M., 2004. Nanoscale structure and mechanical characterization of a natural nanocomposite material: The shell of red abalone. Nano Letters 4, 613–617.

Liao, K., Seam, LI., 2001. Interfacial characteristics of a carbon nanotubes-polystyrene composite system. Applied Physics Letters 79 (25), 4225–4227.

Mallick, P.K., 1997. Composites Engineering Handbook. Marcel Dekker, USA.

Qian, D., Dicdkey, E.C., 2000. Load transfer and deformation mechanisms in carbon nanotube–polystyrene composites. Applied Physics Letters 76 (20), 2868–2870.

Quek, M.Y., 2002. Stress transfer at a partially bonded fibre/matrix interface. International Journal of Adhesion and Adhesives 22, 303–310.

Ruoff, R.S., Lorents, D.C., 1995. Mechanical and thermal properties of carbon nanotubes. Carbon 33 (7), 925–930.

Ruoff, R.S., Lorents, D.C., Dong, Q., Liu, W.K., 2003. Mechanical properties of carbon nanotubes: Theoretical predictions and experimental measurements. Comptes Rendus Physique 4, 993–1008.

Schadler, L.S., Giannaris, S.C., Ajayan, P.M., 1998. Load transfer in carbon nanotube epoxy composites. Applied Physics Letters 73 (26), 3842–3844.

Shen, H.S., 2001. Hygrothermal effects on the postpucking of shear deformable laminated plates. International Journal of Solids and Structures 43, 1259–1281.

Timoshenko, S.P., Goodier, J.N., 1970. Theory of Elasticity, third ed. McGraw-Hill, New York.

Tu, Z.C., Yang, Z.C., 2002. Single walled and multiwalled carbon nanotubes viewed as elastic tubes with the effective Young's moduli dependent on layer number. Physical Review B65, 233407.

Wang, H., Li, Z., 2003a. Diffusive shrinkage of a void within a grain of a stressed polycrstal. Journal of the Mechanics and Physica of Solids 51, 961–976.

Wang, H., Li, Z., 2003b. The instability of the diffusion-controlled grain-boundary void in stresses solid. Acta Mechanica Sinica 19, 330–339.

Wang, H., Li, Z., 2003c. The shrinkage of grain-boundary voids under pressure. Physical Metallurgy and Materials Science 34, 1493–1500.

Wang, H., Li, Z., 2004a. The three-dimensional analysis for diffusive shrinkage of a grain-boundary void in stressed solid. Journal of Materials Science 39, 3425–3432.

Wang, H., Li, Z., 2004b. Stability and shrinkage of a cavity in stressed grain. Journal of Applied Physics 95 (11), 6025–6031.

Wang, H., Li, Z., 2004c. Analytical solution for shape evolution of a coherent precipitate in triaxially stressed solid. Journal of Materials Research 19, 3068–3075.

Wang, X.Y., Wang, X., 2004. Numerical simulation for bending modulus of carbon nanotubes and some explanations for experiment. Composites: Part B 35, 79–864.

Wang, X., Yang, H.K., 2005. Axially critical load of multiwall carbon nanotubes under thermal environment. Journal of Thermal Stresses 28 (2), 185–196.

Wang, X., Zhang, Y.C., Xia, X.H., 2004. C.H. Huang, Effective bending modulus of carbon nanotubes with rippling deformation. International Journal of Solids and Structures 41, 6429–6439.

Wang, X., Wang, X.Y., Xiao, J. A nonlinear analysis of the bending modulus of carbon nanotubes with rippling deformations. Composite Structures, in press.

Yakobson, B.I., Brabec, C.J., Bernholc, J., 1996. Nanomechanics of carbon tubes: Instability beyond linear response. Physical Review Letters 76, 2511–2514.

Zhang, X., Liu, H.Y. et al., 1999. On steady-state fibre pull-out, Part I: The stress field. Composites Science and Technology 59, 2179–2189.